Nb–25%Zr in Strong Magnetic Fields: Magnetic, Resistive, Ultrasonic, and Thermal Behavior

L. J. NEURINGER AND Y. SHAPIRA
National Magnet Laboratory, Massachusetts Institute of Technology, Cambridge, Massachusetts*
(Received 18 March 1966)

Measurements of the magnetization, electrical resistance, ultrasonic attenuation and velocity, and the temperature variation resulting from flux jumps have been carried out on Nb–25%Zr in dc magnetic fields up to 100 kG. The values of the upper critical field H_{c2} obtained from magnetization, resistance, and ultrasonic measurements are compared with each other. The temperature variation of H_{c2} over the interval $1.5°K \leq T \leq T_c$, where $T_c = 10.8°K$, was determined from resistance measurements and the data are compared with the predictions of Maki's theory. It is found that the effects of the Pauli spin paramagnetism on the magnitude and temperature variation of the bulk upper critical field are smaller than those calculated from the theory of Maki. The effects of a magnetic field on the ultrasonic velocity and attenuation in the mixed and normal states of Nb–25%Zr are explained on the basis of the phenomenological theory of Alpher and Rubin. This theory accounts quantitatively for: (1) the attenuation edge of shear and longitudinal waves at H_{c2}, (2) the abrupt change in the velocity of shear waves at H_{c2}, and (3) the effect of a magnetic field on the attenuation of longitudinal and shear waves in the normal state. The Alpher–Rubin theory, although originally derived for impure metals in the *normal* state, also gives a good description of the behavior of ultrasonic waves in the megacycle range propagating in the *mixed state* if the electrical conductivity is taken to be infinite. At higher ultrasonic frequencies, however, deviations from the theory appear in the mixed state. If these deviations are to be explained within the framework of the Alpher–Rubin theory, one must postulate the existence of a finite effective ac resistance, in the mixed state, which is operative at these high frequencies. The data suggest that this ac resistance arises from viscous motion of the flux lines and that it is closely akin to the dc flow resistance. Observations of heating spikes and abrupt changes in the ultrasonic attenuation, which occur in one-to-one correspondence with flux jumps, are reported. Two of the salient features of the observed flux jumps, and the concomitant heating spikes, are their repetitive occurrence at fixed intervals of the magnetic field and the decrease in their relative spacing when the temperature of the sample is lowered. These features are discussed in light of the recent theory of Swartz and Bean for magnetic instabilities in the mixed state of high-field superconductors.

I. INTRODUCTION

DURING the past several years the high-field superconducting alloy Nb–25%Zr has been investigated extensively. To a large extent the aim of these investigations was to study those physical properties of the material which are important for its use in the construction of high-field magnets. However, from the point of view of the fundamental science of superconductors Nb–25%Zr has received comparatively little attention. The research described in this paper centers on fundamental studies of the superconducting properties of Nb–25%Zr. This research covers a wide range of experiments such as magnetization, resistive transitions, ultrasonic attenuation and velocity changes, and magnetic instabilities or flux jumps. Because these various experiments have been performed on the *same* sample, meaningful comparisons can be made between the results of different measurements where they relate to the same property. The many experimental results reported herein are compared with three separate theories which are used to interpret: (a) the magnitude and temperature variation of the upper critical field, (b) the magnetic field dependence of the ultrasonic attenuation and velocity in the mixed and normal states, and (c) the spacing with respect to magnetic field of repetitively occurring flux jumps.

One of the fundamental properties of a type-II superconductor is the bulk upper critical field H_{c2}, which depends on the temperature. Recent experimental investigations[1,2] have shown that for some high-field superconductors the measured upper critical field H_{c2} is lower than the upper critical field H_{c2}* which is calculated on the basis of the Ginzburg-Landau-Abrikosov-Gor'kov (GLAG) theory.[3] The difference between H_{c2} and H_{c2}* was attributed to the Pauli spin paramagnetism whose effect on the upper critical field had not been considered in the original GLAG formulation. Clogston[4] has indicated that the Pauli paramagnetism places an upper limit H_p on the field to which superconductivity can exist. Subsequently, Maki[5] showed by a detailed calculation that the Pauli paramagnetism reduces the value of H_{c2} and modifies its temperature variation. Recently we have reported on experiments designed to test the predictions of Maki's theory.[6] These experiments were carried out on Nb–37 at.%Ti and Nb–56 at.%Ti alloys. For the latter alloy the effect of the Pauli paramagnetism on H_{c2} was large and readily

* Supported by the U. S. Air Force Office of Scientific Research.

[1] T. C. Berlincourt and R. R. Hake, Phys. Rev. **131**, 140 (1963).
[2] Y. B. Kim, C. F. Hempstead, and A. R. Strnad, Phys. Rev. **139**, A1163 (1965).
[3] V. L. Ginzburg and L. D. Landau, Zh. Eksperim. i Teor. Fiz. **20**, 1064 (1950); A. A. Abrikosov, Zh. Eksperim. i Teor. Fiz. **32**, 1442 (1957) [English transl.: Soviet Phys.—JETP **5**, 1174 (1957)]; L. P. Gor'kov, Zh. Eksperim. i Teor. Fiz. **37**, 1407 (1959) [English transl.: Soviet Phys.—JETP **10**, 998 (1960)].
[4] A. M. Clogston, Phys. Rev. Letters **9**, 266 (1962).
[5] K. Maki, Physics **1**, 127 (1964).
[6] Y. Shapira and L. J. Neuringer, Phys. Rev. **140**, A1638 (1965).

observable. It was found that while the Pauli paramagnetism plays a definite role in determining the upper critical field H_{c2}, the theory of Maki overestimates its effects. The study of the Nb-Ti alloys was hampered somewhat by the lack of magnetization data for these materials. The upper critical field was therefore determined solely on the basis of resistive measurements. This shortcoming is present in virtually all previous studies of the upper critical field of high-field superconductors.[7] In the present study of Nb–25%Zr the upper critical field was determined from the magnetization curve, from the resistive transition, and from the ultrasonic attenuation edge. A comparison between the values of H_{c2} obtained by the various techniques is given in Sec. IV where the experimental data are also compared with Maki's theory.

Ultrasonic measurements have been used extensively in the last few years in the investigation of pure elemental superconductors. Studies of ultrasonic propagation in single-crystal low-field superconductors have been numerous[8] and were largely directed at the determination of the BCS energy gap and its anisotropy. In contrast, there has been no experimental or theoretical study of the ultrasonic behavior in high-field superconductors. Recently, the present authors[9] discovered the existence of a distinct attenuation edge, as a function of magnetic field intensity, for ultrasonic shear waves propagating in Nb–25%Zr below the transition temperature T_c. Additional experiments at liquid-helium temperatures revealed[10] that the ultrasonic velocity of shear waves propagating in a parallel magnetic field undergoes an abrupt change at H_{c2}, whereas at lower fields, in the *mixed state*, the velocity was found to increase quadratically with H. This quadratic increase of the ultrasonic velocity in the mixed state was reminiscent of a similar effect which had been previously observed in normal metals.[11] In the case of normal metals the change in sound velocity with magnetic field can be explained by the phenomenological theory of Alpher and Rubin[12] (hereafter AR). The possibility that the AR theory might also explain the results in the mixed state of Nb–25%Zr therefore suggested itself. Accordingly, an extensive series of measurements of the ultrasonic attenuation and velocity was undertaken for the purpose of testing the applicability of the AR theory to sound propagation in the mixed and normal states of Nb–25%Zr. Preliminary results of these experiments[10] indicated that the AR theory gives a quantitative description of the behavior, in the mixed state, of ultrasonic waves in the megacycle range. In addition, this theory also accounts for the changes in the ultrasonic attenuation and velocity at H_{c2}. However, for higher frequency sound waves, deviations from the AR theory appeared in the mixed state. In Sec.V.A, the central assumptions of the AR theory are reviewed and the conditions under which these assumptions are expected to be valid are discussed. Following this, the equations for the changes in the sound velocity and attenuation due to a magnetic field are given. In Secs. V.B, V.C, and V.D the predictions which are based on the AR theory are compared in detail with ultrasonic data obtained in the normal state at $T=77°K$, in the superconducting state, and in the normal state at liquid-helium temperatures ($H>H_{c2}$).

The development of an instability is a common occurrence in high-field superconductors which are exposed to a rapidly changing magnetic field. When this instability occurs, the previously induced shielding currents decrease abruptly with the result that magnetic flux enters the specimen in a discontinuous fashion. This sudden penetration of the magnetic field into the interior of the specimen is known as a flux jump and is generally accompanied by local heating of the sample. In an earlier account[9] we reported the observation of sudden repetitive heating spikes and momentary changes in the amplitude of ultrasonic echoes (in one-to-one correspondence) which occur in the mixed state as the external magnetic field is swept. At that time it was surmised that these heating spikes and ultrasonic attenuation changes were due to flux jumps. In Sec. VI we report the results of *simultaneous* measurements of the sample temperature, variation of the magnetic flux threading the specimen, and changes in the amplitudes of ultrasonic echoes, which prove that the heating spikes and ultrasonic attenuation changes are, in fact, associated with flux jumps. The repetitive occurrence of flux jumps has been observed in tube magnetization studies,[13] in experiments conducted with superconducting wires,[14] and in solid rod samples.[15] The concomitant temperature increases (heating spikes) were discovered independently by the present authors[9] and by Zebouni *et al.*[15] Because high magnetic fields were not available to the latter workers they were not able to observe the persistence of heating spikes throughout the mixed state of high-field Nb-Zr alloys. In contrast, the present

[7] See, for example, Refs. 1 and 2.

[8] D. H. Douglass, Jr., and L. M. Falicov, in *Progress in Low Temperature Physics*, edited by C. J. Gorter (North-Holland Publishing Company, Amsterdam, 1964), Vol. IV, p. 97; N. Tepley, Proc. IEEE **53**, 1586 (1965); A. R. Mackintosh, *Phonons and Phonon Interactions* (W. A. Benjamin, Inc., New York, 1964), p. 181.

[9] L. J. Neuringer and Y. Shapira, Solid State Commun. **2**, 349 (1964).

[10] Y. Shapira and L. J. Neuringer, Phys. Rev. Letters **15**, 724 (1965); **15**, 873(E) (1965).

[11] A. A. Galkin and A. P. Koroliuk, Zh. Eksperim. i Teor. Fiz. **34**, 1025 (1958) [English transl.: Soviet Phys.—JETP **7**, 708 (1958)]; G. A. Alers and P. A. Fleury, Phys. Rev. **129**, 2425 (1963); Y. Shapira, Ph.D. thesis, MIT, 1964 (unpublished).

[12] R. A. Alpher and R. J. Rubin, J. Acoust. Soc. Am. **26**, 452 (1954).

[13] Y. B. Kim, C. F. Hempstead, and A. R. Strnad, Phys. Rev. **129**, 528 (1963); N. Morton, Phys. Letters **19**, 457 (1965).

[14] M. A. R. Leblanc and F. L. Vernon, Jr., Phys. Letters **13**, 291 (1964).

[15] N. H. Zebouni, A. Venkataram, G. N. Rao, C. G. Grenier, and J. M. Reynolds, Phys. Rev. Letters **13**, 606 (1964); R. Hancox, Phys. Letters **16**, 208 (1965).

authors have shown[9] that the heating spikes persist up to the upper critical field of Nb-25%Zr. More recently Claiborne and Einspruch[16] reported the existence of ultrasonic and thermal effects in a Nb-3.6%Zr alloy which are similar to those described in our earlier report.[9]

While previous authors have observed the repetitive occurrence of flux jumps they did not account for the magnitude of the magnetic field interval between successive flux jumps. In Sec. VI the results for the magnetic field interval between adjacent flux jumps, and the dependence of this interval on temperature, are compared with the phenomenological theory of Swartz and Bean[17] for magnetic instabilities in the mixed state of high-field superconductors.

II. EXPERIMENTAL PROCEDURE

All the samples used in the present work were cut from a specimen of unannealed Nb-25%Zr kindly provided by the Westinghouse Corporation. The original specimen was cylindrically shaped, 0.26 in. in diameter and 0.75 in. long. Some of the physical properties of the specimen are listed in Table I.

Magnetization measurements were carried out at liquid-helium temperatures on a cylindrical sample, 0.7 in. long and 0.26 in. in diameter. These measurements were performed by direct integration of the emf induced in a pickup coil surrounding the sample. The sample and pickup coil were immersed directly in the liquid helium and the applied magnetic field **H**, produced by a water-cooled solenoid, was oriented parallel to the axis of the cylindrical sample. The emf induced in the pickup coil is proportional to $d(H+4\pi M)/dt$, where M is the magnetization of the sample. The dH/dt term was suppressed by a series opposing compensating coil wound on the same coil form as the pickup coil but displaced from it by 0.5 in. The two coils straddled the magnetic center of the solenoid symmetrically. In order to achieve full suppression of the dH/dt term an effort was made to make the two coils as identical as possible. Each coil was comprised of 4525 turns of No. 40 AWG magnet wire and was 0.75 in. long with an i.d. of $\frac{9}{16}$ in. A Dymec operational amplifier with capacitive feedback was used to time-integrate the signal from the pickup coils. The output of the integrator was connected to the y input of an x-y recorder and a signal proportional to the current through the magnet was fed to the x input. The magnetic field versus current characteristic of the magnet was measured prior to each run with a Newport type-J flux integrator which had been calibrated against an NMR probe. The accuracy of the magnetic field measurements is estimated to be better than 2%.

[16] L. T. Claiborne and N. G. Einspruch (to be published).

[17] P. S. Swartz and C. P. Bean, General Electric Progress Report No. 4, Contract No. AF-33(657)-11722, 1965, p. 31 (unpublished); P. S. Swartz and C. P. Bean, Bull. Am. Phys. Soc. **10**, 359 (1965).

TABLE I. Physical properties of Nb-25%Zr.

Density at 77°K (g/cm^3)		8.1
Shear velocity at 77°K (10^5 cm/sec)		1.88
Longitudinal velocity at 77°K (10^5 cm/sec)		4.7
Dc resistivity ($\mu\Omega$ cm)	$T=300$°K:	40.4
	77°K:	28.3
	4.2°K:	27.5 ($H>H_{c2}$)
Transition temperature (°K)		10.8±0.2

Resistance measurements at various temperatures were carried out by conventional dc techniques using a four probe arrangement. The sample was a bar, about 6 mm long and 6.2×10^{-3} cm^2 in cross section. Details of the experimental techniques and the apparatus used to regulate and measure the temperature have been previously described.[6]

Ultrasonic attenuation measurements were performed by conventional pulse techniques on the same cylindrical sample used in the magnetization experiments. Acoustical bonds were made with Dow Corning 200 silicone oil having a viscosity of 30 000 centistoke at 25°C. The apparatus used to measure changes in the ultrasonic attenuation in a magnetic field has already been described.[18] In order to measure the absolute magnitude of the change in attenuation it was essential to calibrate the attenuator which is connected between the rf pulse generator and the transducer (cf. Ref. 18, Fig. 1). To obtain a calibration under conditions identical to those during the actual run the calibration was performed immediately following a given run with the sample *in situ*. For this purpose the output of the attenuator, while still connected to the sample-transducer load, was monitored with a Tektronix 545A oscilloscope. By introducing attenuation steps with nominal values of 1 dB, 2 dB, etc., and observing the decrease in the output signal on the oscilloscope, the actual attenuation corresponding to these steps was determined for the given frequency and for the particular acoustical bond used. In general, the large number of observed echoes (10–20) permitted the resolution of a change of $\sim5\times10^{-3}$ dB/cm in the attenuation. The attenuation change was measured to an accuracy of $\sim5\%$.

Changes in the ultrasonic velocity due to the magnetic field were measured by observing the change in the arrival time of the rf signal generated by a particular acoustical echo. For this purpose the rf signal generated by the acoustical echoes in the quartz transducer was amplified and was then fed into a Tektronix 545A oscilloscope. The oscilloscope was triggered by the rf pulse generator and was operated in the "A delayed by B" mode. The rf wave train generated by a particular

[18] Y. Shapira and B. Lax, Phys. Rev. **138**, A1191 (1965).

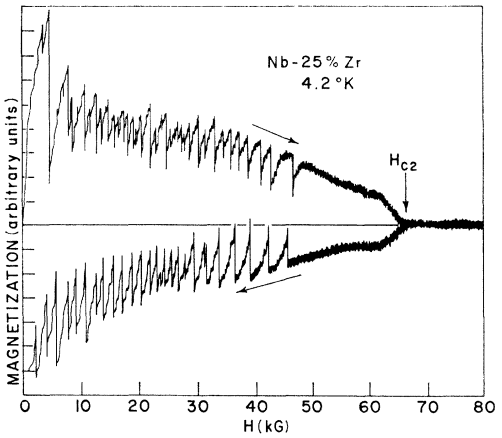

FIG. 1. Recorder tracing of the magnetization of Nb-25%Zr measured at 4.2°K with a sweep rate of 21 kG/min.

acoustical echo was viewed on the oscilloscope. With the time base set to 0.02 μsec/cm, it was possible to observe the motion of the crest or trough of one of the rf oscillations when a magnetic field was applied. The time displacement of the rf signal as a function of H was measured point by point, returning to zero field each time, in order to reduce errors due to drift of the electronic instruments. With this technique a fractional change of $\sim 3\times 10^{-5}$ in the sound velocity could be detected. The measurements were always repeated with an rf wave train generated by a different acoustical echo.

Another phenomenon studied in the present work is the simultaneous appearance of heat pulses and flux jumps. The same sample which was used in the magnetization and ultrasonic experiments was mounted inside a closed copper can which was itself immersed in liquid helium. A small amount of helium exchange gas was introduced into the can to provide thermal contact with the helium bath. A carbon thermometer was mounted on the cylinder sample, and a 2000-turn pickup coil was placed around the sample. The voltage induced in the pickup coil and the voltage developed across the carbon-resistance thermometer were recorded with a two-pen Leeds and Northrup strip chart recorder.

III. MAGNETIZATION

Magnetic properties play a central role in the theory of type-II superconductors. Our present understanding of these superconductors is based, to a large extent upon the GLAG theory.[3] According to this theory there exist two critical fields for type-II superconductors: H_{c1}—the field at which flux starts to penetrate into the sample, and H_{c2}—the field where the transition to the normal state occurs throughout the bulk of the sample. At H_{c2} the magnetic moment of the sample vanishes,[19] in the absence of surface superconductivity.[20] If a superconducting sheath exists on the surface of the sample, the magnetization will not be completely quenched until a field $H_{c3}>H_{c2}$ is reached.[21]

Magnetization measurements were performed at 4.2 and 1.5°K. A recorder tracing of a magnetization curve taken at 4.2°K with a sweep rate of 21 kG/min is shown in Fig. 1. This magnetization curve was obtained immediately after the sample was cooled down from room temperature to 4.2°K in zero magnetic field. Several features of the data in Fig. 1 should be noted: (1) The magnetization curve is irreversible. (2) Repetitively occurring flux jumps appear for both increasing and decreasing magnetic fields. These flux jumps may be due, in part, to the high sweep rate of the applied magnetic field. Measurements[22] of the magnetization of this sample at the relatively low sweep rate of 300 G/min indicated that at this sweep rate flux jumps are less numerous but are not eliminated completely. At 1.5°K and with a sweep rate of 21 kG/min flux jumps persisted almost up to the field where the magnetization dropped below the noise level. (3) The bulk upper critical field H_{c2}, as defined originally by Abrikosov,[23] is obtained directly from the intercept of the magnetization curve with the H axis. It must be noted, however, that while H_{c2} is defined theoretically as the field at which the magnetic moment vanishes, in practice it is possible to follow the magnetization only until it drops below the noise level of the apparatus. In our case H_{c2} was estimated by extrapolating linearly to zero that portion of the magnetization curve which lies above the final knee of the curve. The upper critical field so determined is $H_{c2}=66.2\pm 1$ kG at 4.2°K and $H_{c2}=83.9\pm 2$ kG at 1.5°K. The value of H_{c2} at 4.2°K is in agreement with that reported by Kim, Hempstead, and Strnad.[13] The values of H_{c2} obtained from the magnetization measurements are also in good agreement with the values of the transition field measured by the ultrasonic technique (Sec. V), as may be seen in Fig. 3. This agreement is significant in view of the fact that the ultrasonic technique measures a bulk property. We therefore believe that the magnetic determination of H_{c2} was independent of any effects associated with surface superconductivity.

IV. RESISTIVE BEHAVIOR

A. Results

The variation of the electrical resistance of the Nb-25%Zr alloy with temperature was measured at zero magnetic field using current densities 0.8 A/cm^2 $\leq J\leq$16 A/cm^2. The temperature at which the resistance of the sample becomes one-half of its normal-state

[19] Here we have neglected the susceptibility of the normal state, cf. R. R. Hake, Phys. Rev. Letters **15**, 865 (1965).

[20] D. Saint-James and P. G. de Gennes, Phys. Letters **7**, 306 (1964).

[21] D. J. Sandiford and D. G. Schweitzer, Phys. Letters **13**, 98 (1964).

[22] M. Sauzade and D. B. Montgomery (private communication).

[23] A. A. Abrikosov, Zh. Eksperim. i Teor. Fiz. **32**, 1442 (1957) [English transl.: Soviet Phys.—JETP **5**, 1174 (1957)].

resistance, R_n, was taken to be the transition temperature T_c. The value of T_c was independent of the current density and was measured to be $T_c = 10.8 \pm 0.2$°K. This value is in good agreement with the transition temperatures reported by Hulm and Blaugher[24] and by Wernick *et al.*[25] The width of the superconducting-to-normal resistive transition, defined as the temperature interval over which the resistance changes from 0.1 R_n to 0.9 R_n, was 0.2°K. The normal-state resistivities at various temperatures are listed in Table I.

The electrical resistance as a function of the applied magnetic field intensity H was measured at a fixed temperature. In these measurements J was varied from 8 A/cm² to 1600 A/cm² and **H** was normal to the direction of current flow. Sharp superconducting-to-normal resistive transitions were observed at $T < T_c$ throughout this range of current density. In particular, no gradual increase of the resistance at fields well below H_{c2} (usually associated with flux flow) was observed even at the highest current densities. In this respect the resistive behavior is different from that observed in some other alloys.[2,6,26] A typical example of the superconducting-to-normal resistive transition is shown in Fig. 2 for $J = 110$ A/cm². The width of the transition ($0.1\ R_n < R < 0.9\ R_n$) was ~4.5 kG at 4.2°K and increased slightly when the temperature was lowered. The resistive transition field $H_r(J)$, for a particular J, was taken to be that field at which $R = 0.5\ R_n$. In general, $H_r(J)$ decreased slightly with increasing J. The resistive transition field at zero measuring current $H_r(0)$ was obtained by extrapolating the values of $H_r(J)$ to zero current. The temperature variation of $H_r(0)$ is shown in Fig. 3. As can be seen from this figure the values of $H_r(0)$ are somewhat higher than the values of H_{c2} obtained from the magnetization measurements. Good agreement with the magnetization data are obtained if the onset of resistance at low current densities is used as a criterion for determining the upper critical field. This criterion, which has been used by some workers,[27] depends however, on the sensitivity of the measuring apparatus and on J.[6,26] On the other hand, $H_r(0)$ has a well defined experimental meaning and we shall regard it as the *resistive* transition field. The arbitrary nature of this choice, however, should be borne in mind. It is noteworthy that no magnetoresistance was observed at fields above H_{c2}; at 4.2°K the change in the normal-state resistance between 77 and 94 kG is less than 1%.

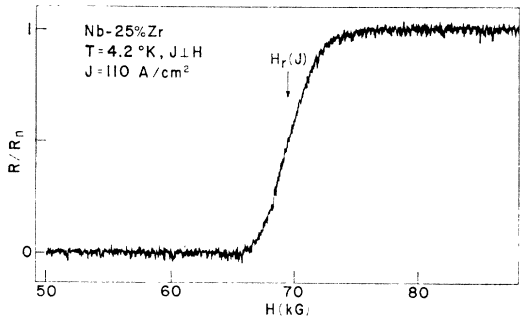

FIG. 2. Electrical resistance R of Nb–25%Zr in a transverse magnetic field at 4.2°K. The resistance has been normalized to its value R_n in the normal state.

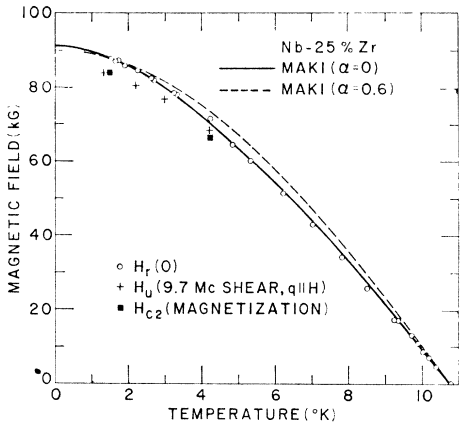

FIG. 3. Temperature variation of $H_r(0)$, H_u, and H_{c2} (magnetization). The theoretical curves are normalized to the value of $H_r(0)$ measured at the lowest temperature.

Another important experimental parameter is the value of the slope of the $H_r(0)$ versus T curve near T_c. Measurements at temperatures just below T_c show that in this range $H_r(0)$ varies linearly with $(T - T_c)$. The value of 124±5 kG was obtained for the temperature derivative $-[dH_r(0)/dt]_{t=1}$, where $t = T/T_c$.

Resistance measurements were also carried out at 4.2 and at 1.5°K with **J**||**H** using current densities 16 A/cm² $\lesssim J \lesssim$ 80 A/cm². These measurements gave results which were similar to those obtained with **J**⊥**H** at the same temperatures and current densities. In particular, the values of $H_r(0)$ obtained when **J**||**H** agreed to within 2% with those obtained when **J**⊥**H**. These results indicate that the effects of surface superconductivity were unimportant in the resistance measurements.

B. Discussion

The temperature and purity dependence of the bulk upper critical field H_{c2} of type-II superconductors has been recently the subject of theoretical investigations. Helfand and Werthamer[28] have presented an exact solution of the linearized Gor'kov equations for H_{c2} as a

[24] J. K. Hulm and R. D. Blaugher, Phys. Rev. **123**, 1569 (1961).
[25] J. H. Wernick, F. J. Morin, F. S. L. Hsu, D. Dorsi, J. P. Maita, and J. E. Kunzler, *High Magnetic Fields* (John Wiley & Sons, Inc., New York, 1962), p. 609.
[26] S. H. Autler, E. S. Rosenblum, and K. H. Gooen, Phys. Rev. Letters **9**, 489 (1962); Rev. Mod. Phys. **36**, 77 (1964); W. DeSorbo, *ibid.* **36**, 90 (1964).
[27] B. S. Chandrasekhar, J. K. Hulm, and C. K. Jones, Phys. Letters **5**, 18 (1963); Rev. Mod. Phys. **36**, 74 (1964).
[28] E. Helfand and N. R. Werthamer, Phys. Rev. Letters **13**, 686 (1964), and to be published.

function of temperature and electron mean free path. In their calculation the effect of the applied magnetic field on the spin magnetic moment of the electron was neglected. Maki[5] has extended his original calculation[29] of H_{c2} to include the effect of the Pauli paramagnetism. Maki's calculations apply only to the case of very short electron mean free path (dirty limit). His results agree with those of Helfand and Werthamer in the dirty limit and in the absence of Pauli paramagnetism.

In order to compare the experimental results with the theoretical predictions, we shall assume that $H_r(0)$ can be identified with the upper critical field H_{c2}. In Fig. 3 the temperature variation of $H_r(0)$ is compared with the temperature variation of H_{c2} as predicted by Maki's theory in the dirty limit and in the absence of any spin paramagnetic effects. The theoretical curve corresponding to the absence of any paramagnetic effect is labelled by $\alpha=0$ and is normalized in such a way that it passes through the value of $H_r(0)$ measured at the lowest temperature. It is evident that this theoretical curve gives the correct shape of the temperature variation of $H_r(0)$ and yields a value of 91.5 kG for $H_r(0)$ at $T=0$.

According to the theories of Helfand and Werthamer, and of Maki the upper critical field at $T=0$, $H_{c2}(T=0)$, in the dirty limit and in the absence of spin paramagnetism is related to the slope $H_0\equiv-(dH_{c2}/dt)_{t=1}$ by the expression

$$H_{c2}(T=0)=0.69H_0. \tag{1}$$

Substituting the experimental value of $-[dH_r(0)/dt]_{t=1}$ $=124\pm5$ kG for H_0, we obtain $H_{c2}(T=0)=85.6\pm3.5$ kG. This value is in reasonable agreement with the value of 91.5 kG for $H_r(0)$ at $T=0$. Still another comparison with theory can be made if we use Maki's expression for $H_{c2}(T=0)$, which, in the dirty limit and in the absence of Pauli paramagnetism, may be written as[2]

$$H_{c2}(T=0)=3.1\times10^4\rho_n\gamma T_c, \tag{2}$$

where $H_{c2}(T=0)$ is in gauss, ρ_n is the normal-state dc resistivity in Ω-cm, γ is the normal-state electronic specific heat coefficient in erg cm^{-3} deg^{-2}, and T_c is the transition temperature in °K. With the values of ρ_n and T_c which are given in Table I and the value[30] $\gamma=26\times10^{-4}$ cal deg^{-2} mole^{-1} we obtain $H_{c2}(T=0)$ $=87.8$ kG, in good agreement with the experimental value of 91.5 kG for $H_r(0)$ at $T=0$. It is noteworthy that the two independent calculations of $H_{c2}(T=0)$, using Eqs. (1) and (2), agree very well with each other although both lie somewhat below the value of $H_r(0)$ at $T=0$. The agreement between theory and experiment is improved if we identify H_{c2} with the field at which the onset of resistance (at low current densities) occurs, or if we use the magnetization value for H_{c2}. Using the magnetization value for H_{c2} we obtain by extrapolation the value $H_{c2}(T=0)=86.5$ kG, in excellent agreement with the values calculated from Eqs. (1) and (2).

The preceding discussion indicates that the effect of the Pauli spin paramagnetism on the magnitude and temperature variation of the bulk upper critical field of Nb–25%Zr is very small. This result is in disagreement with Maki's predictions as can be seen from the following considerations. In Maki's theory the relative importance of the paramagnetic effect is characterized by the parameter α which in the dirty limit may be written as[31]

$$\alpha=3e^2h\gamma/2m\pi^2k^2\sigma_n, \tag{3}$$

where σ_n is the normal-state conductivity in cgs units, e is the electronic charge, m is the free electron mass, and k is the Boltzmann constant. Substituting the known values of these parameters into Eq. (3) we obtain $\alpha=0.62$. In Fig. 3 the theoretical curve for $\alpha=0.6$, taken from Maki's calculations,[32] is compared with the $H_r(0)$ data. As may be seen, this theoretical curve fails to give the correct temperature variation of $H_r(0)$. Moreover, Maki's theory for the effect of the Pauli paramagnetism does not give the proper value of $H_{c2}(T=0)$ as will now be shown. According to Maki, in the presence of the Pauli paramagnetism Eqs. (1) and (2) should be modified to read

$$H_{c2}(T=0)=0.69H_0(1+\alpha^2)^{-1/2}, \tag{4}$$

and

$$H_{c2}(T=0)=3.1\times10^4\rho_n\gamma T_c(1+\alpha^2)^{-1/2}. \tag{5}$$

Substituting the measured value of $-[dH_r(0)/dt]_{t=1}$ for H_0 and $\alpha=0.62$ in Eq. (4) we obtain $H_{c2}(T=0)=72.7$ kG. Equation (5) gives $H_{c2}(T=0)=74.7$ kG. Both of these values are substantially lower than the experimental value of $H_{c2}(T=0)$, thus indicating that the effect of spin paramagnetism in limiting H_{c2} is smaller than that calculated by Maki. The fact that Maki's theory overestimates the effect of the Pauli spin paramagnetism on the upper critical field was noted earlier by the present authors in a study of the Nb-Ti alloys.[6] An explanation of this discrepancy was recently suggested by Werthamer, Helfand, and Hohenberg[31] who considered the effect of spin-orbit scattering. According to these authors the spin-orbit scattering tends to reduce the effect of the Pauli paramagnetism on the upper critical field. (*Note added in proof.* In our more recent experiments on Ti-V, Ti-Nb and Ti-Ta alloys it was found that the deviation of $H_{c2}(t)$ from Maki's predictions increases as the atomic number of the column V constituent increases. These results lend strong support to the hypothesis that spin-orbit scattering counteracts the effect of the Pauli spin paramagnetism on H_{c2}.)

Finally, it should be mentioned that an attempt was made to fit the temperature variation of $H_r(0)$ to

[29] K. Maki, Physics **1**, 21 (1964).
[30] A. El Bindari and M. M. Litvak, J. Appl. Phys. **34**, 2913 (1963), and A. El Bindari (private communication).
[31] N. R. Werthamer, E. Helfand, and P. C. Hohenberg (to be published).
[32] K. Maki (private communication).

several other theoretical models. In particular the following temperature dependences were investigated:[9] (1) Abrikosov: $H_{c2}(t)\sim(1-t^2)$, (2) Abrikosov-Ginzburg: $H_{c2}(t)\sim(1-t^2)/(1+t^2)$, and (3) Gor'kov: $H_{c2}(t)\sim(1.77-0.43t^2+0.07t^4)(1-t^2)$. None of these models reproduced the observed temperature variation of $H_r(0)$. The Gor'kov interpolation formula approached closest to the experimental data, practically coinciding with Maki's curve for $\alpha=0.6$.

V. ULTRASONIC BEHAVIOR

A. Theory

A phenomenological theory for the effects of a magnetic field on ultrasonic propagation in impure normal metals was developed by Alpher and Rubin (AR).[12] This theory was patterned after Anderson's model of ultrasonic propagation in conducting liquids in the presence of a magnetic field.[33] According to AR, the equation of motion of the lattice in a magnetic field may be written as

$$\frac{d^2\xi}{dt^2}=\frac{1}{d}(\mathbf{F}_1+\mathbf{F}_2), \tag{6}$$

where ξ is the ionic displacement, d is the density of the metal, $\mathbf{F}_1$ is the elastic force, and $\mathbf{F}_2$ is the body force exerted on the lattice by the magnetic field $\mathbf{B}$. The elastic force is given by

$$\mathbf{F}_1=\frac{Y}{2(1+\nu)}\left[\nabla^2\xi+\frac{1}{1-2\nu}\nabla(\nabla\cdot\xi)\right], \tag{7}$$

where Y is Young's modulus, and ν is the Poisson ratio. The two basic assumptions made by AR are:

(1) The body force $\mathbf{F}_2$ is related to the current density $\mathbf{J}$, associated with the sound wave, by the equation

$$\mathbf{F}_2=(1/c)(\mathbf{J}\times\mathbf{B}), \tag{8}$$

where $\mathbf{B}$ is the magnetic induction.

(2) The current density $\mathbf{J}$ is given by

$$\mathbf{J}=\sigma\left[\mathbf{E}+(1/c)\left(\frac{d\xi}{dt}\times\mathbf{B}\right)\right], \tag{9}$$

where σ is the electrical conductivity and $\mathbf{E}$ is the electric field associated with the sound wave. The magnetic induction $\mathbf{B}$ is the sum of the dc field $\mathbf{B}_0$ and a small time-periodic magnetic field $\mathbf{b}$ associated with the sound wave.

Starting from Eqs. (6)–(9) and using Maxwell's equations, AR derived expressions for the changes in velocity and attenuation of a longitudinal sound wave in the presence of a transverse magnetic field. In their calculations AR assumed that all quantities associated with the sound wave vary as $e^{i(\omega t-\mathbf{q}\cdot\mathbf{r})}$. Moreover, the equations were linearized so that the results apply only to a small-amplitude sound wave. The theory of AR can be extended to include the explicit dependence of the changes in the ultrasonic velocity and attenuation on the angle θ between the direction of the applied field $\mathbf{H}$ and the wave vector $\mathbf{q}$ of the sound wave. It can be shown that in the presence of a magnetic field the velocity V_l of a longitudinal wave[34] of frequency ω propagating in a metal of permeability μ increases by an amount ΔV_l, where

$$\frac{\Delta V_l}{V_l}=\frac{\mu H^2\sin^2\theta}{8\pi dV_l^2(1+\beta_l^2)},\quad \beta_l=\frac{c^2\omega}{4\pi\sigma\mu V_l^2}. \tag{10}$$

The parameter β_l is related physically to the ratio of the skin depth and ultrasonic wavelength. In addition, the magnetic field causes the amplitude of a longitudinal sound wave to decay with the distance x as $\exp(-\Delta\Gamma_l x)$ where,

$$\Delta\Gamma_l=\frac{\sigma H^2\mu^2\beta_l^2\sin^2\theta}{2dV_lc^2(1+\beta_l^2)}\ (\mathrm{cm}^{-1}.) \tag{11}$$

The total (amplitude) attenuation coefficient is given by the sum $\Gamma_l=\Gamma_{0l}+\Delta\Gamma_l$, where Γ_{0l} is the attenuation in zero magnetic field. The corresponding equations for a shear wave are

$$\frac{\Delta V_s}{V_s}=\frac{\mu H^2\cos^2\theta}{8\pi dV_s^2(1+\beta_s^2)},\quad \beta_s=\frac{c^2\omega}{4\pi\sigma\mu V_s^2}, \tag{12}$$

and

$$\Delta\Gamma_s=\frac{\sigma H^2\mu^2\beta_s^2\cos^2\theta}{2dV_sc^2(1+\beta_s^2)}\ (\mathrm{cm}^{-1}), \tag{13}$$

where V_s is the shear velocity. The total attenuation coefficient of the shear wave is the sum of the attenuation coefficient Γ_{0s} at zero field and $\Delta\Gamma_s$.

While the derivation of Eqs. (10)–(13) proceeds in a straightforward manner from the basic assumptions made by AR, these assumptions are valid only under certain conditions. Specifically, the assumptions contained in Eqs. (8) and (9) are plausible[35] only for a metal with a short electronic mean free path. In such a metal the electrons collide with the lattice within a characteristic distance which is small compared to the sound wavelength, and within a time which is short compared to the cyclotron period and the period of the sound wave. Starting from a microscopic model Rodriguez[36] has shown that Eqs. (10) and (12) are valid when ql, $\omega_c\tau$, $\omega\tau\ll1$, where l is the electronic mean free path,

[33] N. S. Anderson, J. Acoust. Soc. Am. **25**, 529 (1953); For experimental results on liquid mercury see Y. Shapira, Phys. Letters **20**, 604 (1966).

[34] In the presence of a magnetic field the sound waves are not, in general, pure longitudinal or pure shear waves. The mixing of acoustical modes is, however, quite small and can be shown to be unimportant in the present problem.

[35] Y. Shapira, Ph.D. thesis, MIT, 1964 (unpublished).

[36] S. Rodriguez, Phys. Rev. **130**, 1778 (1963).

τ is the electron relaxation time, and ω_c is the cyclotron frequency. Using Eqs. (25) and (27) of Rodriguez' calculation, one can also calculate the (amplitude) attenuation coefficient of a shear wave propagating in a parallel magnetic field ($\theta=0$) when $ql\ll 1$. The result of this calculation is

$$\Delta\Gamma_s=\frac{m^{*2}\beta_s^2(\omega\mp\omega_c)^2\sigma}{2de^2V_s\{[1+(\omega\mp\omega_c)\tau\beta]^2+\beta_s^2\}}, \qquad (14)$$

where the minus and plus signs correspond to right- and left-handed circularly polarized waves, and m^* is the electron effective mass. Equation (14) reduces to Eq. (13) when $\beta\omega_c\tau\ll 1$ and $\omega\ll\omega_c$. One might expect that under the same conditions, i.e., ql, $\beta\omega_c\tau\ll 1$, $\omega\ll\omega_c$, Eqs. (11) and (13) will be valid for an arbitrary angle θ. While this has not been proved theoretically thus far, recent measurements[37] of the attenuation in brass and in silicon-bronze lend strong experimental support to the validity of Eqs. (11) and (13) for arbitrary θ.

Equations (10)–(13) predict the following behavior for the attenuation change $\Delta\Gamma$ and the velocity change ΔV:

(a) Both $\Delta\Gamma$ and ΔV are proportional to H^2.

(b) The maximal effects in $\Delta\Gamma$ and ΔV are attained with $\mathbf{q}\parallel\mathbf{H}$ for shear waves, and with $\mathbf{q}\perp\mathbf{H}$ for longitudinal waves.

(c) $\Delta\Gamma$ should be independent of frequency at high frequencies ($\beta\gg 1$), and vary as ω^2 for low frequencies ($\beta\ll 1$).

(d) As a function of σ, $\Delta\Gamma$ is proportional to σ at low conductivities ($\beta\gg 1$), attains a maximum value when $\beta=1$, and becomes inversely proportional to σ at high conductivities ($\beta\ll 1$). In particular, $\Delta\Gamma=0$ when $\sigma=\infty$.

We proceed to examine the predictions of the AR theory under the assumption that it applies to both the mixed and normal states of a high-field superconductor. Consider first the effect of the magnetic field on the velocity. When $H_{c1}\ll H<H_{c2}$, the material is in the superconducting state ($\sigma=\infty$) and $\mu\approx 1$. In this case the sound velocity should increase as $\Delta V\sim H^2$ and this increase in the velocity should be independent of ω. Near H_{c2} a finite resistivity appears causing the quantity $(1+\beta^2)$ in Eqs. (10) and (12) to increase. As a result the velocity should decrease near H_{c2}. This decrease in ΔV continues until $(1+\beta^2)$ attains its maximum value, that is, when σ becomes equal to its value in the normal state σ_n. At higher fields $(1+\beta^2)$ is constant and ΔV is again proportional to H^2, except that the proportionality constant is smaller than in the superconducting state. It is essential to note that the change in velocity near H_{c2}, which is described here, is due solely to the appearance of a finite resistivity as the magnetic field drives the material into the normal state.

Turning now to the attenuation coefficient we note that the dependence of $\Delta\Gamma$ on σ is governed by the factor $\Delta\Gamma\sim\sigma H^2(1+\beta^{-2})^{-1}$ which appears in Eqs. (11) and (13). Since β is inversely proportional to σ, we conclude that in the superconducting state ($\sigma=\infty$) there should be no attenuation change with magnetic field, i.e., $\Delta\Gamma=0$. With the appearance of a finite resistivity near H_{c2}, the attenuation coefficient should exhibit a rapid increase with field because of the sudden increase in β. The detailed behavior of the rapid increase of $\Delta\Gamma$ near H_{c2} depends on the value of β in the normal state. It was noted earlier that the function $\Delta\Gamma$ versus σ has a maximum when $\beta=1$, that is when $\sigma=c^2\omega/4\pi\mu V^2$, where V is the sound velocity (V_s or V_l). As a consequence, the behavior of the ultrasonic absorption near H_{c2} depends on whether β is smaller or greater than unity in the normal state. If in the normal state β is less than unity, the attenuation will have a simple dependence on H, namely, it will increase abruptly but monotonically with field near H_{c2}, and vary quadratically with H when $H>H_{c2}$. On the other hand, if $\beta>1$ in the normal state, the attenuation will first increase with field near H_{c2}, as resistance starts to develop, and will then reach a maximum when $\beta=1$. Further increase in the field causes the resistance and the parameter β to increase with the result that the attenuation will decrease. Finally, at fields well above H_{c2}, when the conductivity is constant, the attenuation should increase quadratically with H. The new feature which is expected when $\beta>1$ in the normal state is the existence of a finite peak in the attenuation near H_{c2}, in addition to the attenuation edge. In the preceding discussion we have not considered the cases of shear waves in a transverse field, and longitudinal waves in a parallel field, since no changes in the attenuation are expected at H_{c2} in these instances. We have also assumed that the electrical conductivity in the superconducting-to-normal transition region is uniform throughout the sample.

The conventional interpretation[8,38] of the ultrasonic attenuation change near the critical field of superconductors is based on the BCS theory. This theory predicts that the attenuation Γ_S in the superconducting state is lower than the attenuation Γ_N in the normal state. The ratio of Γ_S to Γ_N is related to the temperature-dependent energy gap 2ϵ by the expression

$$\Gamma_S/\Gamma_N=2/[1+\exp(\epsilon/kT)]. \qquad (15)$$

It is important to recognize that Γ_N in Eq. (15) is the attenuation, due to the electrons, that would have been present at zero magnetic field had the material been normal at zero field, and is not the actual attenuation in the normal state at $H>H_{c2}$. The actual attenuation at $H>H_{c2}$ is $(\Delta\Gamma+\Gamma_N)$, where $\Delta\Gamma$ is the increase of the attenuation in the normal state due to the field H

[37] Y. Shapira and L. J. Neuringer, Phys. Letters **20**, 148 (1966).

[38] R. W. Morse, in *Progress in Cryogenics*, edited by K. Mendelssohn (Heywood and Company, Ltd., London, 1959), Vol. I.

[cf. Eqs. (11) and (13)]. We shall show that for Nb–25%Zr at liquid-helium temperatures and at $H>H_{c2}, \Delta\Gamma\gg\Gamma_N$, and hence $\Delta\Gamma\gg(\Gamma_N-\Gamma_S)$. Thus, the effect of the magnetic field on the ultrasonic attenuation is much larger than the difference $(\Gamma_N-\Gamma_S)$ between the intrinsic attenuation (at zero field) in the normal and superconducting states. To compare the magnitude of $\Delta\Gamma$ with Γ_N we consider the case of a shear wave of frequency $\omega=10^8$ sec^{-1} propagating in a parallel magnetic field. We assume that $ql\ll1$ and $\beta_s>1$, as is the case in the normal state of Nb–25%Zr. Equation (13) then becomes

$$\Delta\Gamma_s\cong\sigma H^2\mu^2/2dV_sc^2. \tag{16}$$

Assuming a free-electron metal, Γ_N is given by[38]

$$\Gamma_N=\tfrac{1}{5}m^*E_f\omega^2\sigma/e^2V_s{}^3d, \tag{17}$$

where E_f is the Fermi energy. Equating $\Delta\Gamma$ to Γ_N and substituting the typical values $m^*=9.1\times10^{-28}$ g, $V_s=2\times10^5$ cm/sec, $E_f=5$ eV, and $\mu=1$, we obtain the field H_1 at which $\Delta\Gamma=\Gamma_N$. The calculation gives $H_1=1.7$ kG. It is readily apparent that for Nb–25%Zr at liquid-helium temperatures and at fields above $H_{c2}(H\gtrsim70$ kG) the attenuation change $\Delta\Gamma$ predicted by the AR theory is some 3 orders of magnitude larger than Γ_N. This result proves the contention that attenuation changes observed in Nb–25%Zr near H_{c2} are due primarily to the effect of the magnetic field on the normal attenuation and not to the difference between the intrinsic attenuation $(\Gamma_N-\Gamma_S)$ in the normal and superconducting states. The same conclusion applies to longitudinal waves of frequency $\omega\sim10^8$ sec^{-1} propagating in a transverse magnetic field.

B. Results: $T=77$°K

To test the theoretical predictions of the preceding section, experiments were conducted at 77°K at which temperature the material is in the normal state and the inequalities ql, $\omega\tau,\omega_c\tau$, $\beta\omega_c\tau\ll1$, $\omega\ll\omega_c$ are well satisfied. The attenuation of 4.3- and 14.3-Mc/sec shear waves was measured in dc magnetic fields up to 90 kG. In order to maximize the attenuation change, the magnetic field was oriented along the direction of sound propagation [cf. Eq. (13)]. The experimental results are shown in Fig. 4 together with the theoretical curves which were calculated from Eq. (13) using the parameters listed in Table I. As can be seen there is good agreement between theory and experiment. The values of the parameter $\beta_s{}^2$ for these curves are 2.97 for the 4.3-Mc/sec wave and 33 for the 14.3-Mc/sec wave. Note that the magnitude of $\Delta\Gamma$ is different for the two frequencies, as expected. The results of similar measurements of the attenuation of 12- and 29-Mc/sec longitudinal waves in a transverse magnetic field up to 90 kG were also in accord with the predictions of Eq. (11).

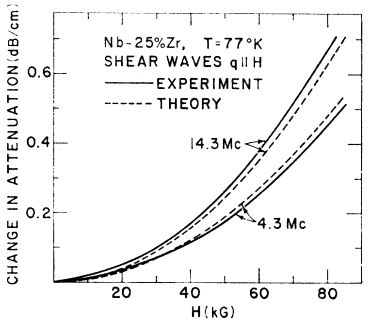

FIG. 4. Change of the ultrasonic attenuation of shear waves propagating in a parallel magnetic field at 77°K. The dashed curves are calculated using Eq. (13).

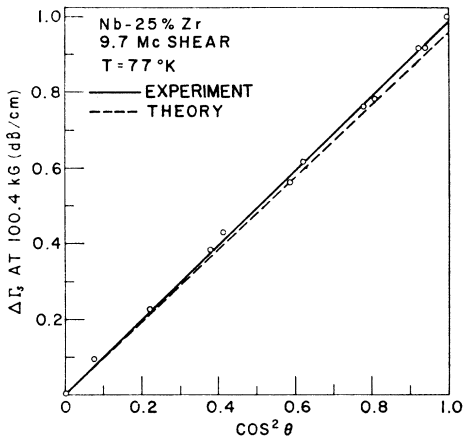

FIG. 5. Angular variation of the attenuation of shear waves caused by a magnetic field of 100.4 kG at 77°K. The circles are the experimental points. The solid line is a straight line drawn through the data points. The dashed line has been calculated using Eq. (13).

Another experimental test of Eqs. (11) and (13) involves the predicted dependence of the attenuation on the angle θ between the direction of sound propagation and the direction of the magnetic field. The angular variation of the attenuation caused by a magnetic field of 100.4 kG is shown in Fig. 5. The circles are the measured values for a 9.7-Mc/sec shear wave and the dashed line is calculated using Eq. (13). The $\sin^2\theta$ dependence of the attenuation change in the case of longitudinal waves was verified for a 29-Mc/sec wave.

The variation of the sound velocity of 4.3-Mc/sec shear waves was measured in a parallel magnetic field. The resultant change $\Delta V_s/V_s$ at 102.3 kG was $\sim4\times10^{-4}$ as compared with the theoretical value of 3.7×10^{-4}.

C. Velocity Changes in a Magnetic Field at $T<T_c$

From Eqs. (10) and (12) it is seen that in order to produce the greatest change in velocity with a given magnetic field one must first choose the proper angular orientation, viz., $\mathbf{q}\|\mathbf{H}$ for shear waves, and $\mathbf{q}\perp\mathbf{H}$ for longitidinal waves. It is further observed that when $\sigma=\infty$, the fractional change in the velocity is inversely proportional to the square of the sound velocity. Since $V_s=0.4V_l$, the maximum fractional velocity change should occur for shear waves propagating parallel to the

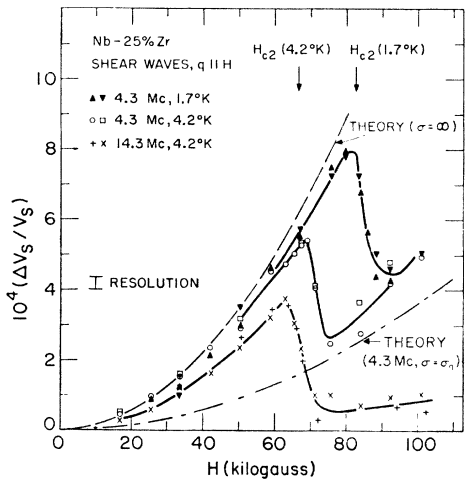

FIG. 6. Change of the ultrasonic velocity of shear waves in a parallel magnetic field. The broken curves are calculated on the basis of Eq. (12). The theoretical curve with $\sigma=\infty$ is independent of the ultrasonic frequency. The theoretical curve with $\sigma=\sigma_n$ is for a 4.3-Mc/sec sound wave.

applied magnetic field. The variation of the sound velocity of 4.3-Mc/sec shear waves as a function of the magnetic field at 4.2 and 1.7°K is shown in Fig. 6. Also shown in this figure are the results for 14.3-Mc/sec shear waves at 4.2°K. Measurements were also made at 4.2°K with 10-Mc/sec waves for which the data points fall between the curves for 4.3- and 14.3-Mc/sec waves.

Several qualitative features of the data should be noted: (1) The two sets of experimental points at a given frequency and temperature, which correspond to measurements of the time delay of two different acoustical echoes, are in good agreement with each other. (2) In the mixed state the sound velocity increases as H^2. (3) The sound velocity decreases abruptly at H_{c2}, as is expected on the basis of the AR theory. The magnetic field at which this abrupt decrease in ΔV_s occurs varies with temperature because H_{c2} is a function of the temperature. (4) At a fixed temperature, an increase in the frequency of the shear wave from 4.3 to 14.3 Mc/sec causes the magnitude of ΔV_s in the mixed state to decrease slightly.

In order to compare experiment and theory, the velocity change in the mixed state predicted by the AR theory [Eq. (12)] is shown in Fig. 6. In constructing the theoretical curve we have set $\sigma=\infty$ (superconducting state) and $\mu=1$. The assumption $\mu=1$ should be valid for $H\gg H_{c1}$, where the magnetic induction **B** is nearly equal to **H**. Under these assumptions Eq. (12) predicts that the velocity change in the mixed state should be independent of the frequency of the sound wave. As Fig. 6 indicates, the data for the 4.3-Mc/sec wave are in good agreement with the AR theory, but the experimental points for the 14.3-Mc/sec shear wave lie somewhat below the theoretical curve. It is noteworthy that the theoretical curve does not involve any adjustable parameters. Interpreted within the framework of the AR theory the results for the 14.3-Mc/sec wave would indicate the existence of a small, but finite, resistivity at fields well below H_{c2}. The existence of such a resistance would then imply the presence of a finite change in attenuation in the mixed state. This conclusion is borne out experimentally, as will be seen in the next section which deals with the attenuation results at $T<T_c$.

The possibility that a finite resistance may exist at $H<H_{c2}$, where the dc resistance is zero, is at first sight puzzling. However, since the sound wave gives rise to alternating currents, one might expect that the ac resistivity (rather than the dc resistivity) is more relevant to the discussion of sound propagation in the mixed state. The resistivity enters Eqs. (10) and (12) via the factor $(1+\beta^2)^{-1}$. Since $\beta\sim\omega$, we expect the effect of this resistance on the sound velocity to be noticeable only when the frequency is sufficiently high so as to make β comparable to unity in the mixed state.

It has been observed experimentally[2,6,26] that in some type-II superconductors the dc resistivity, when measured with moderately high current densities, is nonzero at $H<H_{c2}$. In such instances one defines the flow resistance R_f as the slope of the straight-line portion of the V-I characteristic of the superconductor (cf. Ref 2). This type of resistance is believed to arise from viscous forces which act on the moving flux lines when the Lorentz force on these flux lines exceeds the pinning force. In order to interpret their microwave results, Rosenblum *et al.*[39] have suggested that at microwave frequencies the viscous forces dominate over the pinning forces, even when strong pinning prevents the observation of dc flow-resistance. As a result, the effective resistance at microwave frequencies, even at low current densities, is closely related to the dc flow-resistance of an "ideal" superconductor with no pinning forces. Rosenblum *et al.* have defined a characteristic frequency ω_0 at which the viscous force on a flux line equals the pinning force. For $\omega\gg\omega_0$ the ac resistivity was shown to be equal to the flow resistivity. Typical values of ω_0 were found to lie in the megacycle range.

Turning to the ultrasonic velocity changes *in the mixed state* one expects the assumption $\sigma=\infty$ to be a useful approximation when the ac resistivity is small enough that (in the mixed state) $\beta\ll1$. However, if the ac resistivity is sufficiently high that in the mixed state $\beta\gtrsim1$, the velocity changes should be smaller than those calculated with $\sigma=\infty$. For the present results with shear waves the condition $\beta\ll1$ should be satisfied at low frequencies when $\omega\ll\omega_0$, whereas the condition $\beta\gtrsim1$ should be met at high frequencies when $\omega\gtrsim\omega_0$. It is seen in Fig. 6 that for the 4.3-Mc/sec shear wave the data points do follow the AR curve with $\sigma=\infty$, while for

[39] B. Rosenblum, J. I. Gittleman, and A. Rothwarf, Bull. Am. Phys. Soc. **11**, 106 (1966); J. I. Gittleman and B. Rosenblum, Phys. Rev. Letters **16**, 734 (1966).

the 14.3-Mc/sec wave the data lie below this theoretical curve. This suggests that for shear waves ω_0 is in the 10-Mc/sec range, which is in order of magnitude agreement with values of ω_0 inferred by Rosenblum *et al.* for other type-II superconductors.

In order to interpret the results in the normal state ($H>H_{c2}$) we have plotted in Fig. 6 the theoretical curve for the change in the sound velocity of a 4.3-Mc/sec wave using the normal resistivity. As can be seen, the change $\Delta V_s/V_s$ for the 4.3-Mc/sec shear wave at $H>H_{c2}$ is in reasonable agreement with the prediction of the AR theory. Similar agreement between experiment and theory was found for 10- and 14.3-Mc/sec shear waves. The slight discrepancy between theory and experiment in the normal state is not surprising since similar deviations have been previously observed[11] in other materials when $\beta>1$.

Finally, we discuss further evidence from several control experiments which prove the validity of Eqs. (10) and (12) in describing the velocity changes in a magnetic field. The velocities of 4.3-Mc/sec shear waves and of 10-Mc/sec longitudinal waves, both with $\mathbf{q}\perp\mathbf{H}$, were measured at 4.2°K. As expected, for the shear waves no change in the velocity was observed in fields up to 100 kG. For the longitudinal waves a small change in the velocity with H was observed in the superconducting and normal states. At 84 kG, $\Delta V_l/V_l\sim1.4\times10^{-4}$ which agrees, within experimental accuracy, with the theoretical value $\Delta V_l/V_l=1.1\times10^{-4}$. Because the magnitude of the change in the longitudinal velocity was small, it was not possible to ascertain whether any abrupt change occurred at H_{c2}. In another control experiment the velocity of a 10-Mc/sec longitudinal wave propagating in a parallel magnetic field was measured at 4.2°K. No change was observed up to 100 kG. This result rules out the possibility, within the limits of the experimental resolution, of changes in the length of the specimen as being responsible for the results shown in Fig. 6. It might be suggested that the results in Fig. 6 are due to changes in the elastic moduli between the superconducting and mormal states.[40] However, such an explanation for the present results must be dismissed since the velocity changes are found to depend on the angle between $\mathbf{q}$ and $\mathbf{H}$ and on the ultrasonic frequency. Had the observed velocity changes been due to changes in the elastic moduli they would have been independent of θ and ω. The experimental results indicate therefore that the magnetic field effects predicted by the AR theory dominate the effects of changes in the elastic moduli.

D. Attenuation at $T<T_c$

The attenuation of ~10-Mc/sec shear waves was measured at liquid-helium temperatures in a parallel magnetic field up to 100 kG. An abrupt increase in attenuation appeared near H_{c2}. A typical trace of the attenuation as a function of H at 4.2°K is shown in Fig. 7. The ultrasonic transition field H_u was chosen to be that field at which $AB=BC$ (see Fig. 7). Values of H_u at several temperatures in the liquid-helium range are plotted in Fig. 3. The excellent agreement between H_u and H_{c2} (as determined from the magnetization experiments) indicates that the attenuation edge occurs at the upper critical field. The magnitude of the attenuation edge at 4.2°K was ~0.6 dB/cm, and increased to ~0.8 dB/cm at 1.5°K.

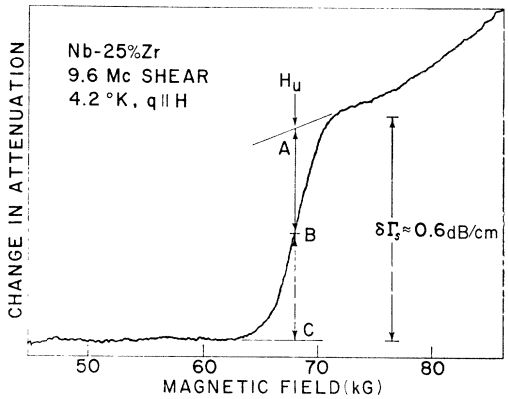

FIG. 7. Recorder tracing of the ultrasonic attenuation edge for 9.6-Mc/sec shear waves propagating in a parallel magnetic field at 4.2°K. H_u is the field where $AB=BC$.

The expected variation of the attenuation coefficient with H at $T<T_c$ has been discussed in Sec. V.A in connection with the AR theory. Qualitatively, the theory predicts the rapid increase of attenuation near H_{c2} which is shown in Fig. 7. In the following discussion further data will be presented concerning the variation of the attenuation change $\delta\Gamma$, defined in Fig. 7, with the angle θ between $\mathbf{q}$ and $\mathbf{H}$ and with the ultrasonic frequency ω. These data will be compared in detail with the predictions of Eqs. (11) and (13). Rather than proceeding directly to a comparison between experiment and theory, we shall begin by describing several experimental observations which remained unexplained for a long time. Only when contact was finally made with the AR theory was it possible to account for these findings.

Soon after the initial discovery of the absorption edge for *shear* waves, further experiments using 10-Mc/sec *longitudinal* waves were carried out at 4.2°K. In these experiments no change in the attenuation with H was observed in the configuration $\mathbf{q}\|\mathbf{H}$ in fields up to 100 kG, while a finite absorption edge was seen at H_{c2} when $\mathbf{q}\perp\mathbf{H}$. Further experiments showed that the magnitude $\delta\Gamma$ of the change in attenuation at H_{c2} for longitudinal waves varied approximately as $\sin^2\theta$. It thus appeared as if the presence of an attenuation edge depended on the direction of particle motion relative to the magnetic field; that is, $\delta\Gamma$ is greatest when the particle motion is perpendicular to $\mathbf{H}$, and is zero when

[40] G. A. Alers and D. L. Waldorf, IBM J. Res. Develop. 6, 89 (1962).

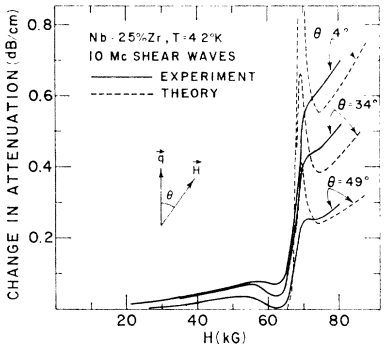

FIG. 8. Angular variation of the attenuation of 10-Mc/sec shear waves, as a function of magnetic field intensity, at 4.2°K. The theoretical curves are calculated from Eq. (13) using the dc resistivity at low-current densities ($J=30$ A/cm^2; $\mathbf{J}\perp\mathbf{H}$).

$\mathbf{q}\|\mathbf{H}$. To test this hypothesis an experiment was performed using 10-Mc/sec shear waves in which the direction of the particle motion was made to lie either in the plane containing $\mathbf{q}$ and $\mathbf{H}$, or always perpendicular to $\mathbf{H}$. The attenuation was then measured as a function of the angle θ between $\mathbf{q}$ and $\mathbf{H}$. In both cases the increase in attenuation $\delta\Gamma$ near H_{c2} was proportional to $\cos^2\theta$ and was found to be independent of the direction of the particle motion relative to $\mathbf{H}$. In particular, with $\mathbf{q}\perp\mathbf{H}$ the absorption edge was absent even when the direction of particle motion was perpendicular to $\mathbf{H}$. The hypothesis that the existence of the absorption edge depends on the direction of particle motion relative to $\mathbf{H}$ was thus disproved. From these results it became apparent that any theory which purports to explain the existence of an absorption edge must also account for the $\sin^2\theta$ and $\cos^2\theta$ dependence of the magnitude of the absorption edge for longitudinal and shear waves, respectively. In addition, for shear waves the theory would have to predict an attenuation coefficient which is independent of the direction of particle motion relative to the magnetic field.

The experiments with shear waves revealed another facet of the problem. The magnitude of $\delta\Gamma$ near H_{c2}, with $\mathbf{q}\|\mathbf{H}$, was virtually independent of the ultrasonic frequency in the range 5 to 25 Mc/sec. This result was puzzling because usually ultrasonic effects in metals increase rapidly with frequency. The BCS expression, Eq. (15), for the difference $(\Gamma_N-\Gamma_S)$ between the attenuation in the normal and superconducting states could not be used to explain the observed angular and frequency dependence of $\delta\Gamma$ near H_{c2}. Using the BCS expression one is led to the conclusions that $\delta\Gamma$ should be independent of θ, and that it should increase rapidly with frequency since Γ_N increases with ω. Both of these conclusions, however, are contradicted by the experimental observations.

All of these seemingly puzzling observations find a natural explanation in the AR theory. In order to compare the observed attenuation change $\delta\Gamma$ at H_{c2} with the AR theory one must first establish the relationship between $\delta\Gamma$ and the attenuation change $\Delta\Gamma$ predicted by this theory. From the arguments of Sec. V.A one expects the difference between the intrinsic attenuation in the normal and superconducting states $(\Gamma_N-\Gamma_S)$ to be negligible compared to the magnitude of $\Delta\Gamma$ in the normal state at $H\geq H_{c2}$. Consequently, $\delta\Gamma$ should be very nearly equal to $\Delta\Gamma$ in the normal state at H_{c2}.

A quantitative test of the predicted field and angular dependence of the attenuation was carried out with 10-Mc/sec shear waves at 4.2°K. The change in attenuation was measured for several different settings of the angle between $\mathbf{q}$ and $\mathbf{H}$. The experimental results are shown in Fig. 8 by the solid lines. The magnitude of the attenuation change $\delta\Gamma$ at H_{c2} is seen to decrease with increasing θ, in agreement with the theory. The position of the absorption edge with respect to magnetic field is invariant to the angle θ, as expected. Also shown in Fig. 8 are theoretical curves calculated by using Eq. (13) and the measured dc resistivity as a function of H at low current densities, ($J=30$ A/cm^2, $\mathbf{J}\perp\mathbf{H}$). It is seen in Fig. 8 that the agreement between theory and experiment is satisfactory except for the failure to observe experimentally the peak in the calculated attenuation. As discussed earlier, the existence of a finite peak in the attenuation near H_{c2} is predicted by Eq. (13) when $\beta_s>1$ in the normal state. One might expect that this peak will be observed with 10-Mc/sec shear waves since $\beta_s=3.9$ in the normal state. However, a necessary condition for detection of the peak in the attenuation is that the electrical conductivity in the superconducting-to-normal transition region does not vary appreciably throughout the sample. It is not clear whether the failure to observe this peak is, in fact, due to a smearing caused by a nonuniform conductivity, although such an hypothesis is the most plausible one at this time. One feature of the experimental data in Fig. 8 which is not predicted by the theory is the existence of a small precursor attenuation at fields well below H_{c2} when $\theta\neq 0$. No such precursor attenuation is observed at 10 Mc/sec when the propagation direction of the shear wave is parallel to the applied magnetic field (cf. Fig. 7). However, at higher frequencies some attenuation is observed for shear waves at $H<H_{c2}$ even when $\mathbf{q}\|\mathbf{H}$.

Considering now the frequency dependence of the attenuation, Eqs. (11) and (13) predict that $\Delta\Gamma$ is proportional to ω^2 at low ultrasonic frequencies ($\beta\ll 1$) but is independent of ω for high frequencies ($\beta\gg 1$). Note that β is inversely proportional to the square of the sound velocity so that at a given frequency β_s is larger than β_l. For example, at a frequency of 10 Mc/sec ($T=4.2$°K, $H>H_{c2}$) $\beta_s^2=15$, whereas $\beta_l^2=0.39$. Hence, for shear waves $\Delta\Gamma_s$ should be virtually frequency-independent above 10 Mc/sec, whereas in the case of longitudinal waves $\Delta\Gamma_l$ is still strongly frequency-dependent in the range 10 to 30 Mc/sec. The observation that the magnitude of the attenuation jump $\delta\Gamma$ at H_{c2} for shear waves depends only slightly on frequency in the range 5 to 25 Mc/sec is therefore explained by the AR theory.

At frequencies above $\sim$25 Mc/sec, and with $\mathbf{q}\|\mathbf{H}$, a

precursor attenuation is observed for shear waves at fields well below H_{c2}. This precursor attenuation is not expected on the basis of the AR theory if the resistivity in the mixed state is taken to be zero. The possibility that a small but finite effective ac resistivity may be present at $H<H_{c2}$ has already been mentioned in the discussion of the velocity changes. In that discussion it was also suggested that this effective ac resistivity might have the same origin as the dc flow-resistivity which is observed in the mixed state of some type-II superconductors. Further support for the conjecture about the similarity between the dc flow-resistivity and the effective ac resistivity, which appears in ultrasonic measurements at high frequencies, will now be cited.

The presence of a precursor attenuation in the mixed state is evident for shear waves propagating in a parallel magnetic field only at frequencies exceeding $\sim$25 Mc/sec. In the case of longitudinal waves propagating in a transverse magnetic field, however, such a precursor attenuation is already noticeable at 9.5 Mc/sec. The results of measurements of the attenuation of 9.5- and 29.2-Mc/sec longitudinal waves in a transverse magnetic field are shown in Fig. 9. The main features of these data are the appearance of a precursor attenuation at fields well below H_{c2}, the decrease in attenuation at fields just below H_{c2}, and the sudden increase in attenuation at H_{c2}. A similar behavior of the attenuation of longitudinal waves has been observed in Nb-Ti alloys.[6] It is interesting to compare the data in Fig. 9 with the results of dc resistance measurements, performed with moderately high current densities, on alloys in which flow-resistance is observed (cf. Ref. 6, Fig. 1 the curve for $J=150$ A/cm^2). In such measurements a finite resistance which increases monotonically with H is observed in the mixed state. At fields just below H_{c2} the resistance drops, passes through a minimum, and then increases to its normal value at H_{c2}. The similarity of this resistive behavior with the ultrasonic-attenuation results shown in Fig. 9 is striking and suggests a common origin to both phenomena. In view of this similarity one might expect that at high ultrasonic frequencies ($\omega\gg\omega_0$) the effective ac resistivity will be close to the dc flow resistivity[2] $\rho_f=\rho_n H/H_{c2}(T=0)$. It is remarkable that the magnitude of the precursor attenuation in the mixed state, at $H\lesssim 55$ kG, for both 9.5- and 29.2-Mc/sec longitudinal waves (Fig. 9) is, in fact, accounted for by the AR theory if one lets $\rho=\rho_f$. This is not the case, however, for the results with shear waves. [*Note added in proof.* The ultrasonic attenuation of 8 to 56 Mc/sec shear and longitudinal waves has recently been measured by the authors in a well annealed Ti-V alloy ($\omega_0\sim 10^6$ sec^{-1}). It was found that the attenuation in the mixed state is accounted for by the AR theory provided one lets $\rho=\rho_f$.]

In conclusion, it appears that for low-frequency sound waves the effective ac resistivity in the mixed state is sufficiently small that, to a good approximation, one can substitute $\sigma=\infty$ in the formulas of the AR theory. However, as the ultrasonic frequency is increased, a finite effective ac resistivity, which is believed to be associated with viscous motion of the flux lines,[39] must be introduced into the theory.

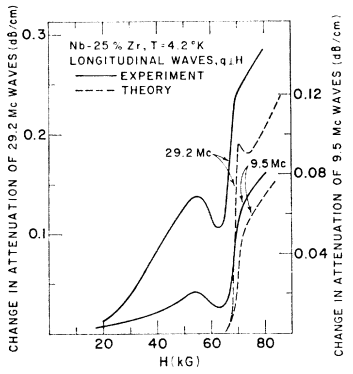

FIG. 9. Ultrasonic attenuation of 9.5- and 29.2-Mc/sec longitudinal waves propagating in a perpendicular magnetic field at 4.2°K. The theoretical curves are calculated from Eq. (11) using the dc resistivity at low current densities ($J=30$ A/cm^2; $\mathbf{J}\perp\mathbf{H}$). Note that the ordinate scales for the two frequencies are different.

VI. FLUX JUMPS

Measurements of the sample temperature, variation of the magnetic flux threading the specimen, and changes in the amplitudes of ultrasonic echoes were carried out simultaneously in a uniformly changing magnetic field. These experiments were performed at $\sim$4.2 and at $\sim$2°K in a magnetic field up to 100 kG. The specimen was mounted in a copper can which was immersed in liquid helium. Some helium gas was introduced into the can to provide thermal contact between the specimen and the helium bath. The sweep rates of the applied magnetic field ranged from 5 to 17 kG/min. No heat or electrical currents were applied to the sample during the course of these measurements.

Figure 10 shows a trace taken with a two-pen recorder of the sample temperature and of the voltage developed across a 2000-turn pickup coil surrrounding the sample. The rate of change of the applied field in this case was 17 kG/min, and the temperature of the helium bath was 4.2°K. It is evident that the flux jumps (detected by the pickup coil) occur in one-to-one correspondence with the thermal pulses, or heating spikes, of the sample. Figure 10 exhibits the temperature variation only for a limited range of magnetic field. When the entire accessible field range is examined, the temperature behavior of the sample is as follows: The sample which is at some ambient temperature T_0 begins to warm up smoothly when the field is switched on and heating spikes appear at a field of several kilogauss. These heating spikes occur repetitively throughout the mixed state and disappear just before the sample is driven into the normal state at H_{c2}. Subsequently, when the magnetic field is decreased towards zero, after it has reached the maximum value attainable with the

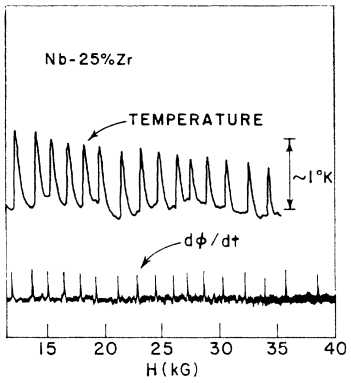

FIG. 10. Trace of a two-pen recorder showing the temperature variation of the sample with magnetic field (upper curve), and the voltage induced in a pickup coil wound around the sample (lower curve). The external magnetic field is increasing at a rate of 17 kG/min. The bath temperature is 4.2°K.

magnet, the heating spikes appear again at $H<H_{c2}$. Once the magnetic field reaches zero and is switched off, the sample returns to its initial temperature T_0.

Several other features revealed by these experiments are worth noting: (1) Whereas the temperature of the sample always increases when a flux jump occurs, independent of whether the applied field is increasing or decreasing, the voltage induced in the pickup coil by a flux jump changes its sign upon reversal of the field sweep. The latter observation is explained by the fact that the sample has an irreversible magnetization curve (Fig. 1). The voltage induced in the pickup coil is proportional to $\dot{\varphi}$, where $\dot{\varphi}$ is the time rate of change of magnetic flux threading the sample. In the presence of an increasing magnetic field a flux jump corresponds to sudden flux penetration ($\dot{\varphi}>0$), whereas in a decreasing field a flux jump corresponds to the sudden exclusion of trapped flux ($\dot{\varphi}<0$). (2) The amplitude and duration of the voltage pulses across the pickup coil, as observed on an oscilloscope, were found to vary somewhat from pulse to pulse. Nevertheless, the following typical values can be regarded as representative: amplitude ~2 V, time duration ~2 msec. Similar results have been reported by Leblanc and Vernon.[14] (3) The duration of the voltage pulse across the pickup coil is much shorter than the duration of the temperature rise, as may be seen from Fig. 10. (4) The rise time of a heating spike is short as compared to its decay time. This is probably due to the rather poor thermal contact between the sample and the helium bath. (5) The number of flux jumps occurring within a given field interval remains essentially constant when the field sweep rate is changed from 17 to 5 kG/min. (6) As the ambient temperature T_0 of the sample is lowered, with the sweep rate of the magnetic field maintained constant, the field interval between successive flux jumps decreases. Thus at ~4.6°K the average spacing in Fig. 10 is 1.6 kG, whereas at ~2.5°K the spacing is 1.2 kG.[9]

The amplitude of ultrasonic echoes was also measured simultaneously with the temperature of the sample. The measurements were performed with 10-Mc/sec shear waves propagating in a parallel magnetic field. The experimental conditions were similar to those described in the preceding paragraphs. It was observed that the amplitude of any acoustical echo undergoes a momentary change whenever a heating spike (flux jump) occurs. Our measurements indicate, however, that these changes in the amplitude of the acoustical echoes cannot be attributed solely to a change in the ultrasonic attenuation in the sample. Had these amplitude changes been due to a genuine change in the ultrasonic attenuation in the sample, the reduction in amplitude of the mth echo, expressed in nepers, would have been proportional to m. However, the observations indicate that this is not the case. Moreover, it was found that the amplitudes of some echoes increase when a flux jump occurs, whereas the amplitudes of others decrease. This behavior is not understood at present. It is conceivable that the temperature rise which accompanies the flux jump not only changes the attenuation in the sample but also warms the acoustical bond between the transducer and the sample thereby changing the insertion loss.

Two of the salient features of the observed flux jumps are their repetitive occurrence at fixed intervals of the magnetic field, and the decrease in their relative spacing when the temperature of the sample is lowered. While previous authors have observed the repetitive occurrence of flux jumps in tube magnetization studies,[13] and in experiments conducted with coils of superconducting wire[14] and with solid-rod samples,[15] they did not account for the observed succession of flux jumps. On the other hand, we find that the present results are accounted for by a recent theory of magnetic instabilities in high-field superconductors developed by Swartz and Bean.[17] A result similar to that obtained by Swartz and Bean has been stated, without derivation, by Wipf and Lubell.[41] However, the formulas of Swartz and Bean are in a more convenient form for comparison of the data with theory.

Swartz and Bean consider a semi-infinite superconducting slab which is cooled in a magnetic field directed parallel to its surface plane. The *external* magnetic field is then assumed to be increased in an isothermal fashion by an amount ΔH. At this point the external field is suddenly increased by a finite amount δH in a time short compared to the thermal diffusion time and long as compared to the electromagnetic diffusion time. This latter increase in field, δH, which is "adiabatic," causes an amount of flux $\delta\varphi$ to penetrate into the sample. The physical quantity of interest is $\delta\varphi/\delta H$ which is defined as the "adiabatic incremental susceptibility." According to Swartz and Bean the first possibility for a flux jump occurs when this suscepti-

[41] S. L. Wipf and M. S. Lubell, Phys. Letters **16**, 103 (1965).

bility becomes infinite. The calculation of the adiabatic susceptibility rests on the following two assumptions:

(1) The superconductor is in the critical state[42] immediately prior to the occurrence of a flux jump.

(2) The increase in temperature $\delta T(x)$ of a volume element located a distance x beneath the surface of the superconductor is given by

$$C\delta T(x)=\tfrac{1}{10}J_c\delta\varphi(x), \tag{18}$$

where C is the specific heat in erg/cm³ °K, J_c is the critical current density in A/cm², and $\delta\varphi(x)$ is the increase in the flux (in maxwells) which threads the portion of the slab lying a distance greater than x from the surface.

With these assumptions it is shown that the adiabatic incremental susceptibility is given by

$$\delta\varphi/\delta H=\lambda\tan(\delta/\lambda), \tag{19}$$

where

$$\frac{1}{\lambda}=\left[\frac{-4\pi\times10^{-2}J_c(\partial J_c/\partial T)}{C}\right]^{1/2}, \tag{20}$$

and

$$\delta=10\Delta H/4\pi J_c. \tag{21}$$

From Eq. (19) it is seen that the first possibility for a flux jump arises when $\delta\varphi/\delta H\to\infty$ i.e., when $\delta/\lambda=\pi/2$. Therefore, a *necessary* condition for an instability to occur is that the field outside the sample exceeds the field deep within the sample by an amount ΔH_{FJ} where

$$\Delta H_{FJ}=[-\pi^3CJ_c/(\partial J_c/\partial T)]^{1/2}. \tag{22}$$

In order to compare the predictions of Eq. (22) with experiment in a quantitative fashion, one must know the specific heat C and temperature variation of the critical current density J_c. For the specific heat we shall make use of the data of El Bindari and Litvak.[30] The situation with regard to the temperature variation of J_c for Nb-25%Zr is not as clear cut. There is experimental evidence[43,44] which indicates that $J_c(T)$ is approximately linear in T, i.e.,

$$J_c(T)=J_c(0)(1-T/T_c), \tag{23}$$

and we shall assume this functional dependence of J_c upon T. Substituting Eq. (23) into Eq. (22) we obtain the following instability criterion

$$\Delta H_{FJ}=[\pi^3C(T_c-T)]^{1/2}, \tag{24}$$

where ΔH_{FJ} is in gauss. Since at temperatures well below T_c the specific heat C decreases rapidly with decreasing temperature, the quantity ΔH_{FJ} is expected to decrease when the temperature is lowered. This prediction is borne out experimentally. In Table II we have presented a comparison between the flux jump spacing observed experimentally and the value of ΔH_{FJ} calculated from Eq. (24). It is seen that the agreement is quite satisfactory, although the observed spacing is somewhat smaller than predicted by Eq. (24). From Fig. 1 it is seen that the magnetic moment of the sample immediately after the occurrence of a flux jump is not zero, which indicates that the field deep within the sample is not equal to the external field. According to Swartz and Bean, a flux jump may occur only when the difference between the external field and the internal field deep within the sample is as large as that given by Eq. (24). If the difference between these two fields immediately following a flux jump is h, then the minimum spacing between flux jumps should be $(\Delta H_{FJ}-h)\leq\Delta H_{FJ}$. Thus, the observed spacing can be smaller than predicted by Eq. (24) when the flux jumps are incomplete.

TABLE II. Comparison between theory and experiment for the spacing between flux jumps.

Temperature (°K)	Observed spacing (kG)	Calculated ΔH_{FJ}, [Eq. (24)] (kG)
4.6	1.6	2.1
2.5	1.2	1.3

It must be recognized that in order for the equations derived above to be applicable, the increment δH must be applied adiabatically. To ensure this adiabatic condition it is necessary for the thermal diffusivity D_{th} to be much smaller than the magnetic diffusivity D_{mag}. These parameters are given by[17]

$$D_{th}=\kappa/C(\text{cm}^2/\text{sec}), \tag{25}$$

$$D_{mag}=10^9\rho_f/4\pi(\text{cm}^2/\text{sec}), \tag{26}$$

where κ is the thermal conductivity in erg/sec cm°K, and ρ_f is the flow resistivity in Ω cm. Various experiments[2] indicate that $\rho_f=\rho_nH/H_{c2}^*(T=0)$ where ρ_n is the normal resistivity. For Nb-25%Zr at 4.2°K, $D_{th}\sim1$ cm²/sec.[45] Using a value of 90 kG for $H^*_{c2}(T=0)$ it is seen that D_{mag} is greater than D_{th} if the applied field is greater than ~40 G. Thus, for the fields used in the present experiments the flux lines can diffuse through the material in a time short compared to the thermal diffusion time and long compared to the magnetic relaxation time, so that the adiabatic assumption is valid.

In the model proposed by Swartz and Bean the rate of change of the applied magnetic field is not considered. While this model gives a satisfactory account of the observed spacing between flux jumps in Nb-25%Zr when the external magnetic field is rapidly varying (5 to 17 kG/min), it does not predict the observed spacing at much slower sweep rates.[22] A more complete

[42] C. P. Bean, Phys. Rev. Letters 8, 250 (1962); Rev. Mod. Phys. 36, 31 (1964).

[43] Y. B. Kim, C. F. Hempstead, and A. R. Strnad, Phys. Rev. Letters 9, 306 (1962).

[44] R. D. Cummings and W. N. Latham, J. Appl. Phys. 36, 2971 (1965), and W. N. Latham (private communication).

[45] S. L. Wipf (private communication).

theory must therefore consider the effect of the rate of change of the external magnetic field. Moreover, Eq. (22) which gives a *necessary* condition for the occurrence of a flux jump must be supplemented by *sufficient* conditions.

VII. CONCLUSIONS

The bulk upper critical field H_{c2} was determined using ultrasonic techniques, in addition to the conventional resistance and magnetization measurements. The values of H_{c2} obtained from these three types of measurements were compared to each other, and the limitations of each of these procedures in obtaining *accurate* values for H_{c2} were pointed out. In the present study the field at which the onset of resistance (at low current densities) occurs was found to be very close to the value of H_{c2} determined from magnetization measurements. A detailed comparison of the temperature variation of H_{c2} with the predictions of Maki's theory shows that this theory overestimates the effects of the Pauli spin paramagnetism. This discrepancy is probably due to the effect of spin-orbit scattering which was neglected by Maki.

It has been shown that the effects of a magnetic field on the ultrasonic propagation in the mixed and normal states of Nb–25%Zr are very large. Extensive data on ultrasonic measurements were interpreted on the basis of the phenomenological theory of Alpher and Rubin. The results for frequencies in the megacycle range are accounted for by assuming that the conductivity in the mixed state is very high so that to a good approximation one may substitute $\sigma = \infty$ in the formulas of the AR theory. However, the ultrasonic behavior at higher frequencies indicates the presence of a finite effective ac resistance in the mixed state. This resistance in the mixed state is supposed to arise from viscous motion of the flux lines, even in the presence of strong pinning forces.

Instability phenomena in the mixed state were investigated using magnetic, thermal, and ultrasonic techniques. The results have been compared with the phenomenological theory of Swartz and Bean. Although this theory accounts for the spacing between successive flux jumps when the external field changes rapidly, a more extensive treatment which includes the effect of the field sweep rate is needed for a fuller understanding of the results.

ACKNOWLEDGMENTS

We are indebted to Y. Iwasa and D. B. Montgomery for their collaboration in the magnetization measurements, and to B. Schwartz and S. Foner for critical reading of the manuscript. We also wish to express our thanks to P. S. Swartz, C. P. Bean, S. L. Wipf, and A. El Bindari for several helpful discussions. The technical assistance of B. Perry, M. Kelly, and W. Tice throughout the course of this investigation is greatly appreciated.